Scientific Research Publishing

Open Journal of Geology, 2024, 14, 1-18
https://www.scirp.org/journal/ojg
ISSN Online: 2161-7589
ISSN Print: 2161-7570

Characteristics of Gold Mineralization at the Baguiomo Gold Panning Site, Koudougou Region, Burkina Faso, West Africa

Pascal Ouiya[1,2*], Aziz Fayçal Tarnagda[2], Martial Eric Fozing[3]

[1]Ecole Normale Supérieure (ENS), Institut Sciences et Technologie (IST), Ouagadougou, Burkina Faso
[2]Laboratoire Géosciences et Environnement (LaGE), Earth Sciences Department, Ouagadougou, Burkina Faso
[3]Department of Geology, University of Dschang, Dschang, Cameroon
Email: *pascal.ouiya@gmail.com

How to cite this paper: Ouiya, P., Tarnagda, A.F. and Fozing, M.E. (2024) Characteristics of Gold Mineralization at the Baguiomo Gold Panning Site, Koudougou Region, Burkina Faso, West Africa. *Open Journal of Geology*, **14**, 1-18.
https://doi.org/10.4236/ojg.2024.141001

Received: November 24, 2023
Accepted: January 2, 2024
Published: January 5, 2024

Abstract

The Birimian Baguiomo formations are located in the northern part of the Boromo greenstone belt. In this belt, the volcanic rocks (tholeiitic basalt, calc-alkaline basalt, andesite) hosting the gold mineralization are located in the Kwademen-Baguiomo shear zone. This mineralization, located only a few kilometers from the Kwademen gold deposit, is uncharacterized and, together with the latter, could constitute a gold potential capable of being economically exploitable. It is in this sense that this work is carried out with a view to characterizing the gold mineralization of the Baguiomo gold panning site. To carry out this work, we have made direct field measurements, combined with microstructures, and combined all this with data from geochemical rock analysis of the basalts that are the main host formations. Geochemical data show that tholeitic basalts formed from a mantle plume that was emplaced in an oceanic plateau context. Calc-alkaline basalts and andesites are comparable to Paleoproterozoic tholeitic basalts (PTH3), which are slightly enriched in light rare earths. Fertility tests show that these basalts concentrate between 3 and 6 ppb of gold at the time of accretion, which is sufficient for remobilization of this primary gold during the Eburnian orogeny to yield a deposit of around 4 - 5 Moz. Gold mineralization is associated with pyrite crystals when the latter are disseminated in the rock mass, whereas it is associated with hematite in quartz veins concordant with S1 shear deformation. It is mainly the pyrite crystals in the pressure shadows that contain the gold grains, whose development would be synchronous with micro-shear zone reactivation during the first phase of $D1_B$ deformation. The second phase of $D2_B$ deformation, which is a crenulation or fracture schistosity, does not significantly affect the shear deformation that controls mineralization.

Keywords

Kwademen-Baguiomo Shear Zone, Gold Panning Site, Gold Mineralization, Eburnian Orogeny

1. Introduction

Burkina Faso, like the Man/Léo Ridge, is rich in gold and base metal deposits (**Figure 1**) located in greenstone belts ([1]-[6]). In these greenstone belts, the various deposits identified are contained in shear zones ([1] [2] [3] [7] [8] [9] [10]). Gold and base metal mineralization is linked to the circulation of hydrothermal fluids, which interact with the surrounding rocks to crystallize new minerals. This mineralogical assemblage, closely linked to hydrothermal alteration, is at the origin of the concentration of numerous deposits, especially gold deposits in orogenic settings ([1] [11] [12]).

Two styles of mineralization are distinguished across the craton: disseminated gold mineralization with high tonnage and low grade, and quartz vein-hosted mineralization with low tonnage and high grade ([13] [14] [15] [16]). In the first type, gold is contained in disseminated sulfides and distributed throughout the host rock mass, whereas in the second type, gold is generally in the form of free gold or included in sulfides.

The Boromo greenstone belt is known for its gold and base metal potential, and includes the Poura, Bissa gold, Kalsaka, Konkéra, Torkéra and Nassara gold deposits, the Perkoa zinc deposit, the Diénéméra-Gongondy copper porphyry and the Kwademen gold deposit. The present study was carried out in the Baguiomo area, around 25 km from Koudougou and 15 km from Tenado (**Figure 2**). The aim of this study is to characterize the Baguiomo gold mineralization in terms of deformation and hydrothermal alteration. To do this, we combined direct field measurements with microstructures and metallography, all coupled with total rock geochemistry data. The data are discussed and compared with other gold deposits.

2. Geological Context

As with the Man/Léo dorsal, the west-central region is formed by formations of Paleoproterozoic age, also known as Birimian formations ([17]). These formations are organized in greenstone belts alternating with vast batholiths of granitoids of the tonalite, trondhjemite and granodiorite (TTG) series ([18] [19]). The greenstone belts and batholiths (TTG) are subsequently intruded by granitoids of various compositions, with calc-alkaline to alkaline affinity ([20] [21] [22] [23]). These greenstone belts are composed of ultrabasite, pillow lava basalt with tholeiitic affinity and andesite, which make up the volcanic unit. This volcanic unit is surmounted by the volcano-sedimentary to sedimentary unit formed of sediments intercalated with basic to intermediate volcanic dykes with calc-alkaline affinity, such as dacites, rhyodacites and rhyolites ([8] [24] [25] [26] [27] [28]).

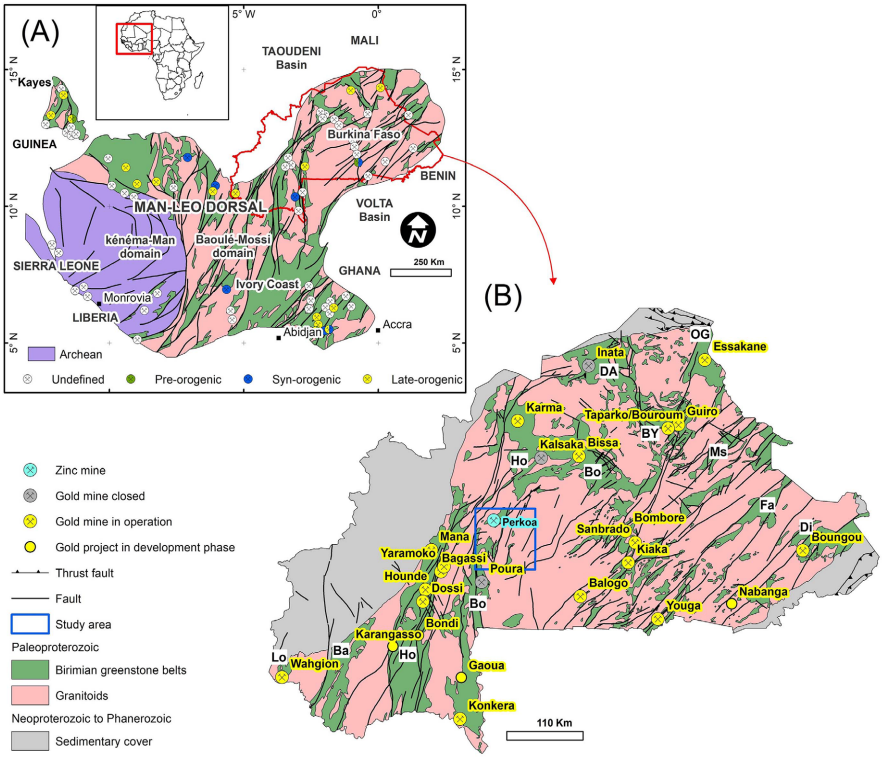

Figure 1. (A) Simplified lithostructural and metallogenic map of the modified Léo Ridge, (B) Lithostructural and metallogenic map of Burkina Faso showing the position of the various deposits; the study area is shown in blue.

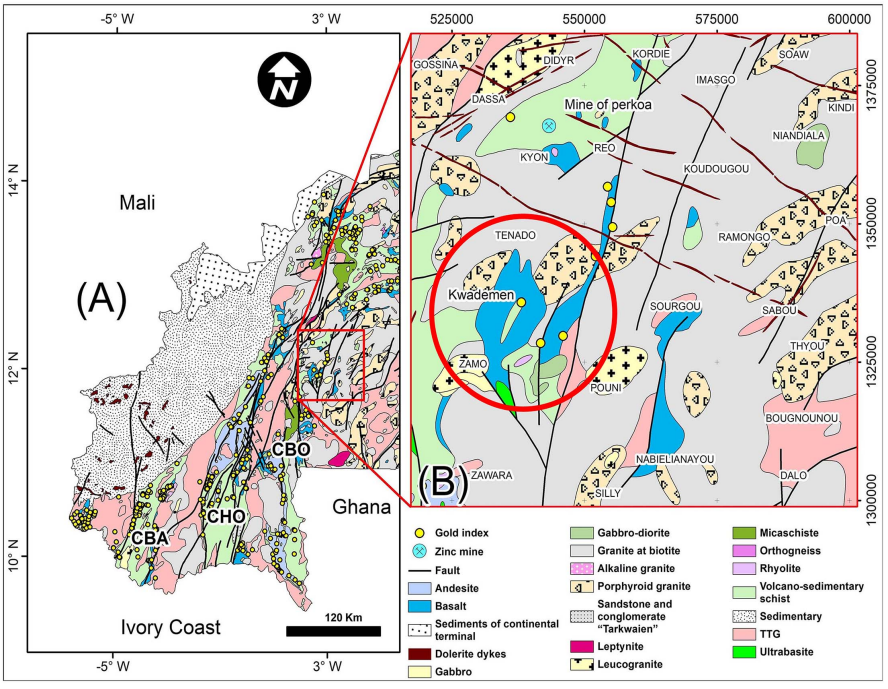

Figure 2. Lithological map of the study area (modified from Castaing *et al.*, 2003). (A) simplified geological map of Burkina with gold mineralization showings, (B) geological map of the study area showing the location of the Kwademen and Baguiomo gold deposits and many other showings.

These formations are affected by polyphase deformation ranging from D1 through D2 to D3 ([23] [28] [29]). The first phase of deformation (D1), marked by general NW-SE shortening orients the structures in a NE-SW to N-S direction. The second and third deformation phases (D2-D3) are responsible for the N-S to NE-SW shear zones. The Baguiomo gold mineralization is located in the northern part of the Boromo greenstone belt, where the formations are mainly volcanic, volcanosedimentary and sedimentary (**Figure 3**). From all the work in the area, it emerges that the Tenado zone, which includes the Baguiomo area, is formed of basalt, andesite and rhyolite, which are associated with pyroclastites (volcanic breccia of andesitic nature, tuffs) and sediments (graphitic, argillite, chert) ([7] [28] [30]).

This ensemble is cut by late gabbro, dolerite and microdiorite dykes. The work of ([7]) shows that the Kwademen formations are affected by ductile deformation (D1) developed under greenschist facies conditions underlined by S1 schistosity with an average orientation of NNE-SSW. The second phase of deformation is a ductile-breaking to brittle deformation marked by an S2 crenulation schistosity.

3. Methodology

The methodology used to arrive at our results was divided into two phases: the field phase and the laboratory phase. The field work consisted of direct measurements of structures directly visible in the field, using a compass and a clinometer. During the field phase, we collected rock samples brought up by gold miners and many other outcrops. The laboratory phase involved making a dozen mine slides for the various studies (petrographic, microstructural, metallographic).

For geochemistry, a set of four (04) samples were selected, some crushed and the rest ground into a fine powder at BUMIGEB (Bureau des Mines et de la Géologie du Burkina). The powders from the various samples were packaged in vials, labelled and sent for analysis. Major and trace elements were analyzed using ICP-AES (Inductively Coupled Plasma Atomic Emission Spectrometry) at ACME analytical laboratories Vancouver Ltd.

4. Results

4.1. Geochemical Data from Baguiomo Basalts

The rocks hosting the mineralization are basalts and basaltic andesites. The basalts contain 50.5 to 50.9 wt.% SiO_2, 12.7 to 12.9 wt.% Fe_2O_3, 4.5 to 5.5 wt.% MgO and 1.1 to 1.2 wt.% TiO_2. The values for calc-alkaline basalts and andesites are respectively 54 and 55 wt.% SiO_2, 9.6 and 11.5 wt.% Fe_2O_3, and 0.6 to 1.2 wt.% TiO_2 and 3.8 wt.% MgO for each. Analytical data showing the different trends of tholeiitic basalts, calc-alkaline basalts and andesites are reported in **Table 1**.

In the TAS diagram of ([31]), our data are housed in the field of basalts and andesitic basalts (**Figure 3(A)**). Basaltic andesites are found to be calc-alkaline

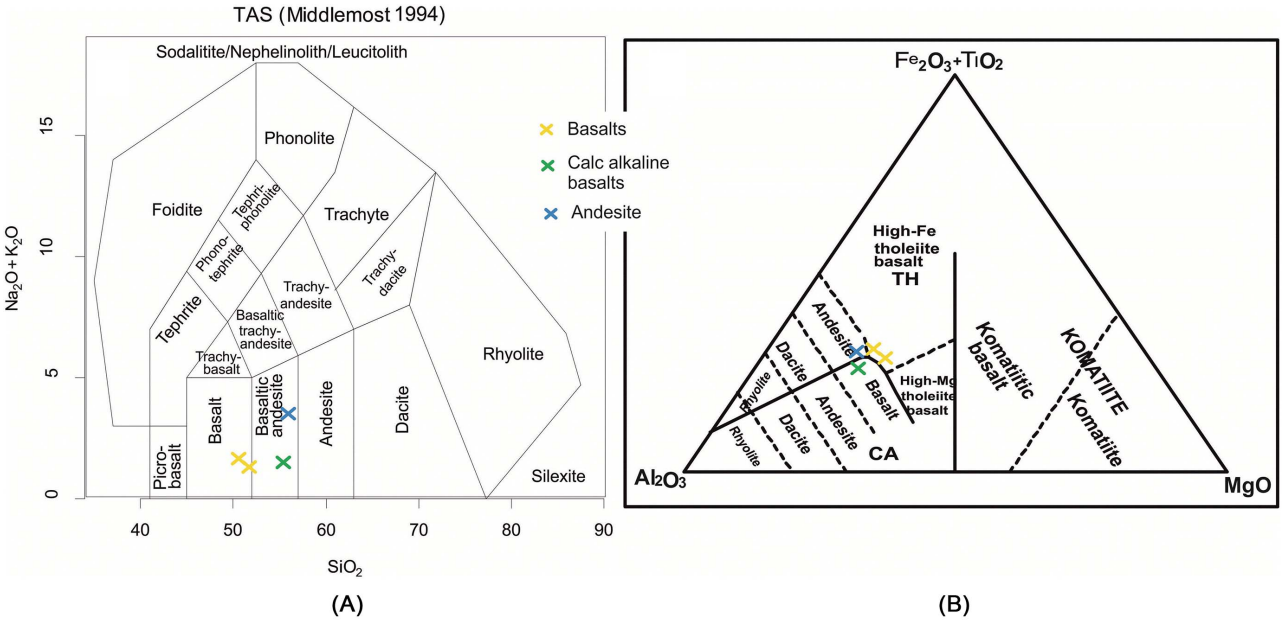

Figure 3. Discrimination diagram for Baguiomo volcanic rocks. (A) SiO_2 vs. $Na_2O + K_2O$ naming diagram showing the fields of tholeithic basalt (yellow cross), calc-alkaline basalt (green cross) and andesite (blue cross) rocks from Baguiomo ([31]); (B) Diagram showing the affinities of Baguiomo volcanic rocks ([32]).

Table 1. Representative major (wt%) and trace (ppm) elements compositions for the Baguiomo basalts, calc akaline basalt and andesites rocks.

SAMPLE	Ba_1	Ba_2	CA-Ba	And
Major elements (wt%)				
SiO_2	50.9	50.5	54	55
TiO_2	1.1	1.2	0.6	1.2
Al_2O_3	14.2	15.2	13.7	14.7
Fe_2O_3	12.7	12.9	9.6	11.5
MnO	0.2	0.2	0.2	0.2
MgO	4.5	5.5	3.8	3.8
CaO	13.1	12.4	13.6	8.5
Na_2O	1.3	1.4	1.3	3.2
K_2O	0.1	0.2	0.2	0.3
P_2O_5	0.1	0.1	0.1	0.1
LOI	1.9	0.5	2.8	1.4
Total	98.1	99.5	97.2	98.6
Traces elements (ppm)				
Rb	4.5	3.4	9.9	8
Ba	394	61	46	184
Sr	163.1	191.9	313.4	290.6
Th	0.5	0.2	1.4	1.7

Continued

U	0.2	<0.1	0.4	0.5
Ta	0.3	0.3	0.4	0.3
Nb	3.4	3.2	4.1	4.1
Hf	1.6	1.9	2.3	3.1
Zr	55	65.7	82.6	111.3
Sc	37.9	24.7	22.3	17.4
La	6.7	4	11.4	12.6
Ce	9.4	9.9	22.9	24.2
Pr	2.1	1.6	3.2	3.1
Nd	10.3	8.9	13.9	13.8
Sm	2.9	2.6	2.8	3.4
Eu	1	1.1	0.9	1
Gd	3.9	3.8	3.4	3.7
Tb	0.7	0.6	0.6	0.7
Dy	4.3	4.2	3.8	3.6
Ho	0.9	1	0.8	0.9
Er	2.7	2.9	2.5	2.9
Yb	2.5	2.8	2.5	2.8
Lu	0.4	0.4	0.4	0.4
Eu/Eu*	0.90	1.03	0.85	0.84
$(La/Yb)_N$	1.81	0.99	3.15	3.06
$(La/Sm)_N$	1.45	0.96	2.55	2.32
Au	6 ppb	3 ppb	5 ppb	5 ppb

Ba = basalt; CA-Ba = calc akaline basalt; And = andesite.

basalts (green cross) and andesites (blue cross) in the AFM diagram by ([32]) (**Figure 3(B)**). Tholeiitic basalts are weakly enriched in iron in the same diagram. In ([33]) diagram, tholeiitic basalts, calc-alkaline basalts and Baguiomo andesites are all placed in the field of tholeiitic lavas (**Figure 4(A)**), as are the other Paleoproterozoic tholeiitic basalts of the West African craton ([28] [34]).

Rare earth spectra normalized to chondrite in the diagram of ([35]) show relatively flat spectra for tholeiitic basalts (La/SmN = 0.96 - 1.45; La/YbN = 0.99 - 1.81), with low europium values (0.90 - 1.03) suggesting an absence of fractionation (**Figure 4(B)**). In the same diagram, rare-earth spectra for andesites and calc-alkaline basalts show a flat profile for heavy rare earths and low enrichment in light rare earths (8 - 9 × chondrite; La/SmN = 2.33 - 2.55; **Figure 4(B)**). The tholeitic basalts from Baguiomo display the same common characters of oceanic plateau-derived basalts already studied in the West African craton ([34] [36]). Calc-alkaline basalts and andesites are comparable to Paleoproterozoic tholeitic

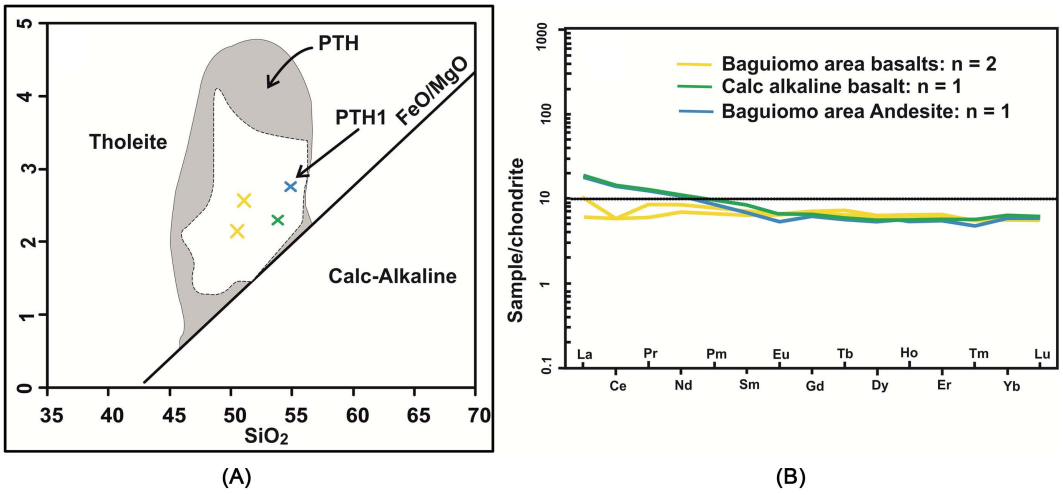

Figure 4. Magmatic affinity diagrams of Baguiomo volcanic rocks. (A) Positions of Baguiomo volcanic rocks on the Feo/MgO Vs. SiO_2 diagram ([33]) also showing the field of the Paleoproterozoic tholeiitic series (PTH1) of the West African craton according to ([34]); (B) Rare earth element diagram normalized to chondrite for Baguiomo volcanic rocks ([35]).

basalts ([34]). The negative europium anomaly in calc-alkaline basalt and andesite could signify feldspar fractionation.

4.2. Mineralized Body Structures

The Baguiomo mineralized zone is a gold panning site several kilometers long and around 1 km wide. The mineralization is hosted mainly by basalts, volcano-sediments (volcanic breccia of andesitic nature) and sediments (**Figure 5**). These host rocks are intersected by late Gabbros dykes in the southern part and by granite in the western part.

Apart from the gabbro, all the formations are affected by two phases of deformation. The first phase of deformation at the Baguiomo scale, called $D1_B$, is a shearing deformation developed under greenschist facies conditions. The S1 schistosity that marks this deformation is fairly penetrative, with a direction varying from N-S to NNE-SSW. Dips are steep to sub-vertical. Generally speaking, the average direction is N0˚E/75W. The second phase of deformation, $D2_B$, is a brittle deformation that repeats the first phase of deformation, $D1_B$. The S2 schistosity that marks this deformation is locally ductile-cracking with a variable orientation in the N96˚E/80˚NE and N46˚E/75NW directions. The orbedded quartz vein is concordant with the S1 schistosity (**Figure 6(A)**). Microscopically, the first phase of alteration is highlighted by biotite, chlorite and iron oxide (**Figure 6(B)**, **Figure 6(C)**). The second phase of deformation is highlighted by carbonate-filled fractures (**Figure 6(D)**).

4.3. Hydrothermal Alteration of Host Formations

The formations hosting the mineralization are affected by hydrothermal circulation of variable intensity. These are essentially basalts and andesitic basalts. In distal zones, hydrothermal alteration is of low intensity in volcanic rocks (basalts,

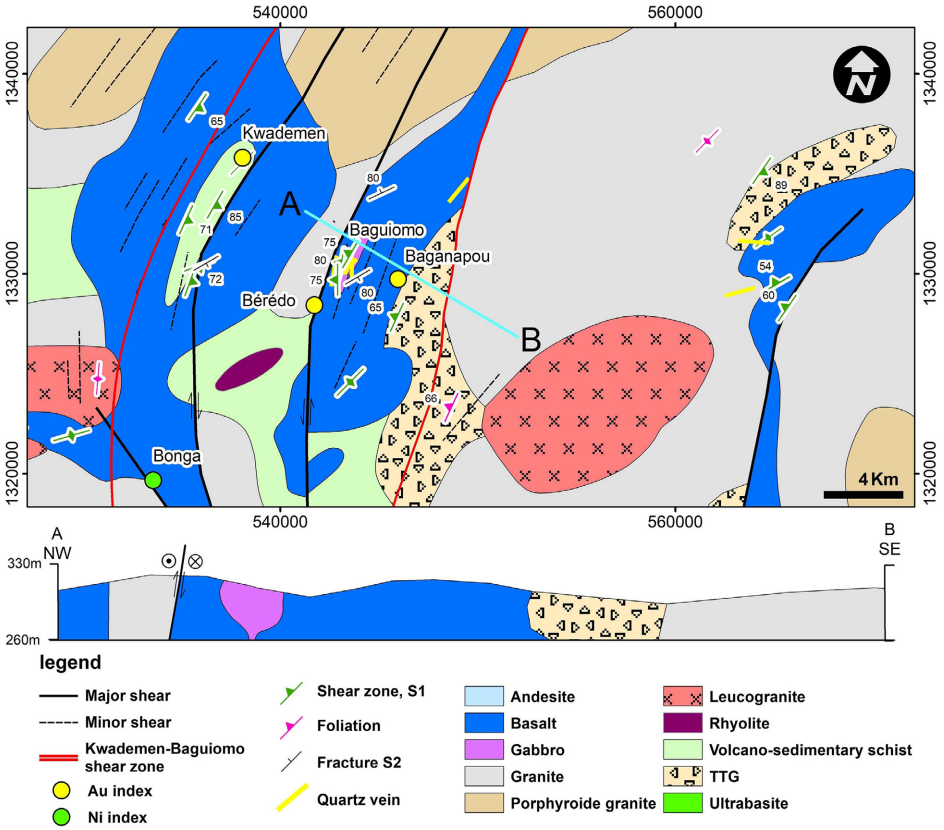

Figure 5. Litho-structural map of Baguiomo showing the various deformation structures affecting the different formations. The Kwademen and Baguiomo gold deposits are contained within the Kwademen-Baguiomo shear corridor (red lines).

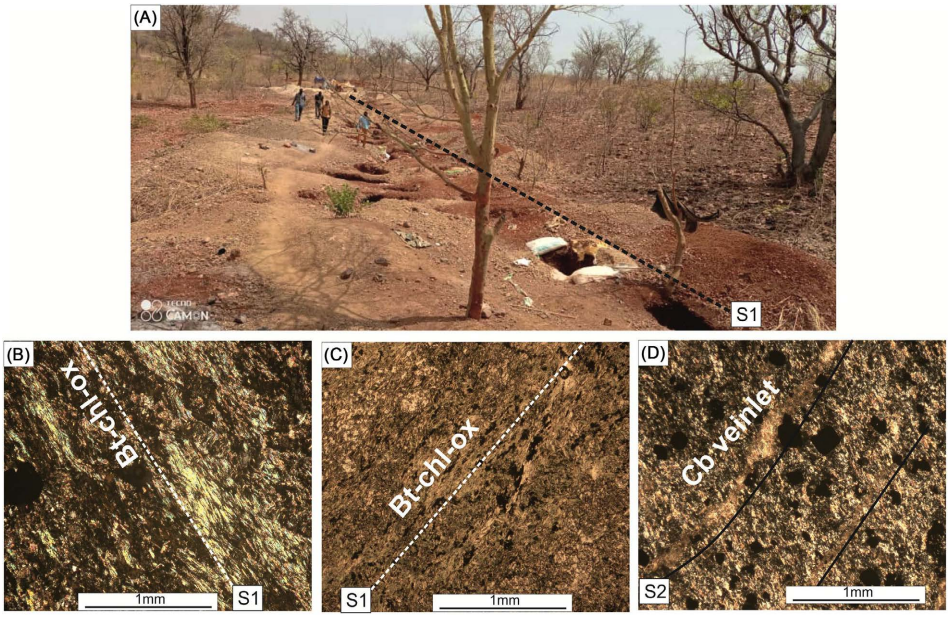

Figure 6. Photograph and microphotographs showing the different deformation structures affecting the mineralized zone. (A) Photograph showing gold pits following S1 shear deformation; (B) S1 shear deformation underlined by biotite-chlorite and oxides; (C) Image seen in natural light of b; (D) Image showing carbonate-filled microfractures underlining S2.

andesitic basalts) (Figure 7(A)). The resulting paragenesis is the mineralogical association of biotite-chlorite-carbonate-iron oxide ± quartz ± pyrite (Figures 7(B)-(D)).

This first phase of alteration is superimposed by moderate silicification with disseminated pyrite crystals (Figure 8(A)). The mineral association characterizing this paragenesis is carbonate-quartz-white mica-pyrite-pyrrhotite ± chlorite (Figure 8(B), Figure 8(C)). This silicification phase is accompanied by a pyritization phase (Figure 8(D)) that develops at the expense of the carbonates (Figure 8(E)). The difference in competence between the matrix and the pyrite crystals causes the latter to rotate during $D1_B$ deformation, creating pressure shadows. These pressure shadows around the pyrite crystals are quartz-filled (Figure 8(F)).

The last phase of hydrothermal alteration is intense silicification (Figure 9(A)). In the field, this is reflected in a quartz vein concordant with the S1 schistosity, where gold-panning activity is intense. This vein is impregnated with oxide and pyrite-Au. Microscopically, the mineralogical association that characterizes this alteration is quartz-oxide-pyrite-carbonate-white mica (Figure 9(B), Figure 9(C)). These oxides may be hematite, as shown in Figure 9(A).

4.4. Gold Mineralization

Gold mineralization at Baguiomo is linked to pyrite crystals that are disseminated

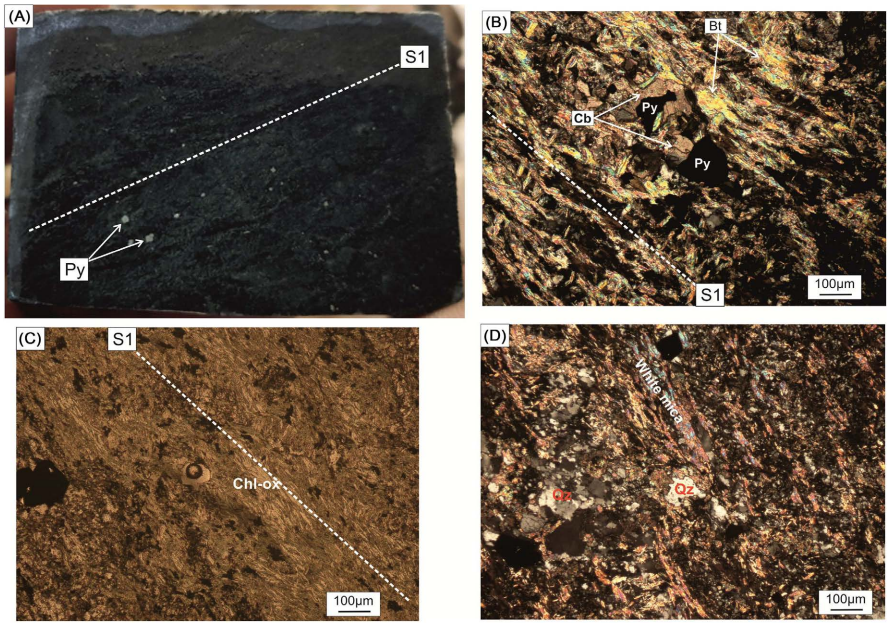

Figure 7. Microphotographs showing the paragenesis of low-silicified basalt. (A) Photograph of a basalt weakly affected by hydrothermal alteration with a few disseminated pyrite crystals; (B) image seen in analyzed and polarized light of a biotite-rich S1 shear band, with pyrite crystals developing at the expense of carbonates, probably ankerite; (C) image seen in natural light showing the S1 highlighted by biotite, chlorite and oxides, (D) image seen in analyzed and polarized light showing weak silica impregnation in the basalt. The biotites are locally transformed into white mica.

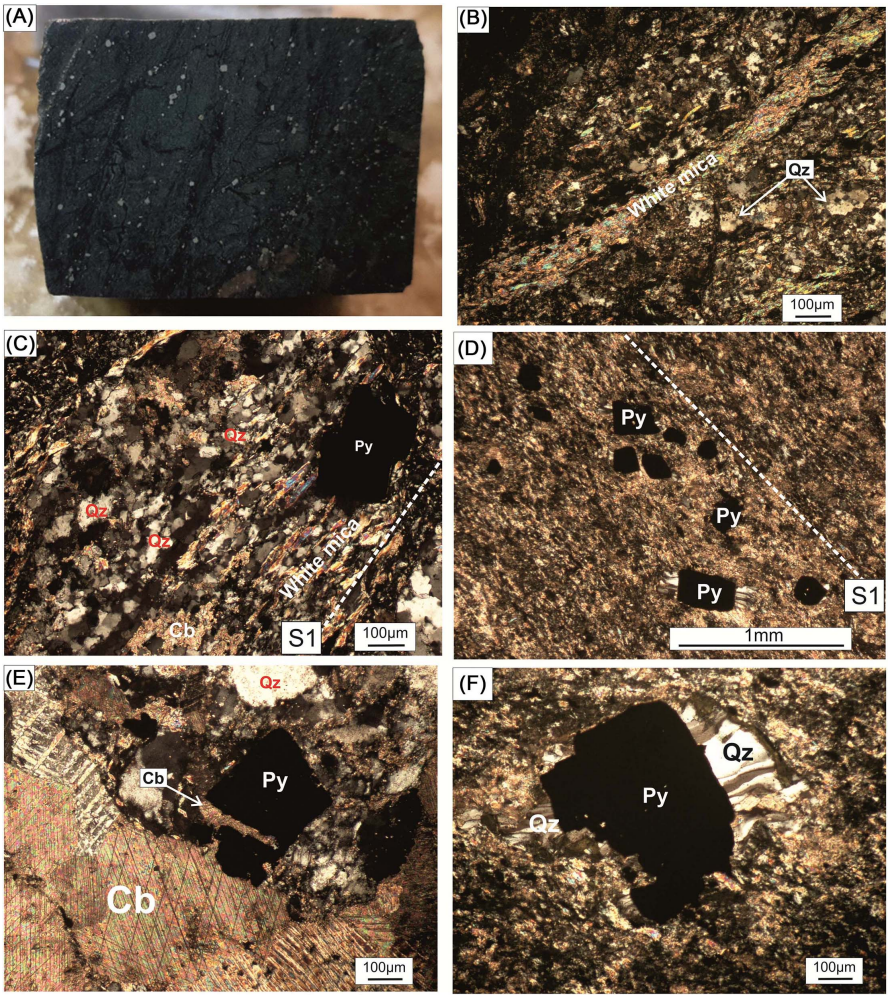

Figure 8. Microphotographs showing the paragenesis of moderately silicified basalt. (A) Photograph of a basalt affected by hydrothermal alteration with pyrite crystals disseminated in the rock mass; (B) image showing a white mica band in a quartz, white mica and carbonate matrix; (C) pyrite crystal taken in a white mica-rich shear band; (D) Aggregate of pyrite crystals arranged in the plane of the S1 schistosity; (E) Pyrite crystal replacing carbonate, probably ankerite; (F) Pressure shadow around a pyrite crystal with fibrous quartz filling.

in the rock mass within andesitic basalts and basalts. Of all the sulfides (pyrite, pyrrhotite) identified in the mineralized zone, gold is linked to pyrite crystals when the latter are dispersed throughout the rock mass, whatever the nature of the host rock (**Figures 10(A)-(D)**). It is the pyrite crystals around which pressure shadows parallel to S1 develop that contain the gold mineralization (**Figure 10(A)**, **Figure 10(C)**).

In the gold-bearing quartz vein, gold is bound to reddish hematite (**Figure 10(E)**). Hematite may also result from the destabilization of pyrrhotite (**Figure 10(F)**). Gold in pyrite crystals occupies microfractures (**Figure 10(D)**), precipitates from pyrite crystal faces (**Figure 10(B)**) or coexists with hematite. Their sizes range from micrometers to a few micrometers (**Figure 10(B)**, **Figure 10(D)**, **Figure 10(E)**).

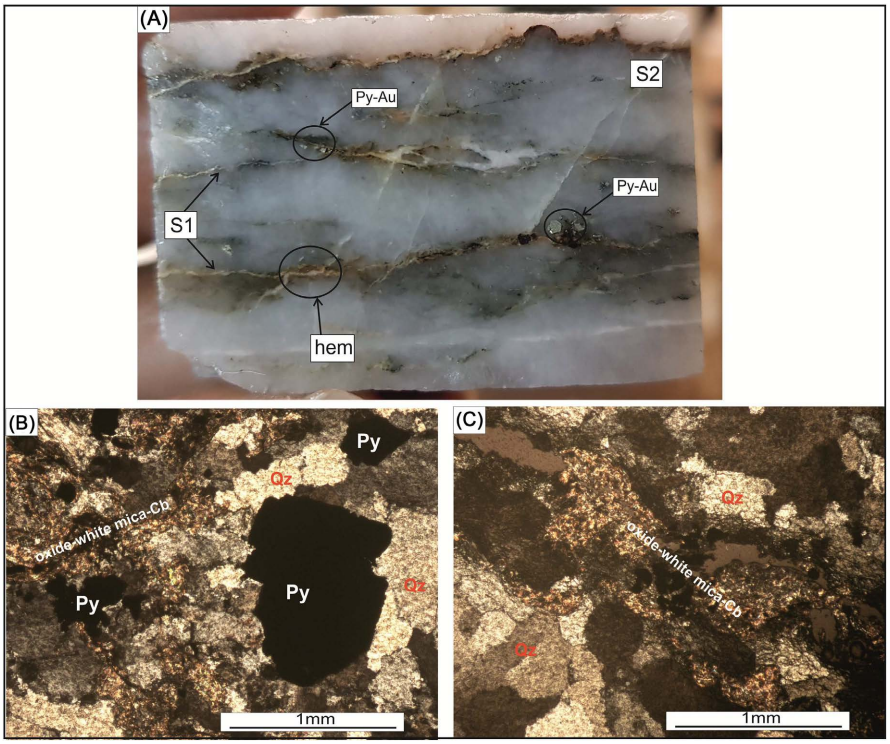

Figure 9. Photograph and microphotographs showing the minerals in the orbedded quartz vein ore. (A) Photograph of the oxide and pyrite-injected quartz vein following the S1, which is locally taken up by the S2; (B) (C) The various minerals in the quartz vein ore.

5. Discussion

The Baguiomo gold mineralization is hosted by basaltic formations that were strongly sheared during the first phase of $D1_B$ deformation marked by S1. This deformation is taken up by a second phase of deformation $D2_B$ which is a fracture schistosity S2.

Geochemical data show that these basalts would have been emplaced in an oceanic plateau setting like the Paleoproterozoic basalts ([30] [34] [36]). They are compatible with iron-enriched Paleoproterozoic tholeiitic basalts (PTH1) emanating from a mantle plume eruption in an oceanic plateau around 2250 to 2200 Ma ([34]). This would prove that the tholeiitic basalts of the Baguiomo region originate from a mantle plume erupted from an oceanic plateau. It has been shown that most large orogenic gold deposits and provinces are related to mantle plume activity ([15] [36] [37] [38]). It is therefore primary gold in these basalts that is remobilized and then precipitated as a deposit in shear zones, referring to the work of ([39]).

Indeed, fertility tests for Baguiomo basalts range from 3 - 6 ppb. Studies have shown that to form a deposit the size of 1 Moz, 19 km^3 of tholeiitic basalts with 1 ppb of primary mineralization are required ([40]). Based on this principle, a gold deposit of between 4 and 5 Moz can be formed in the Baguiomo area, which is more than sufficient for an industrial operation.

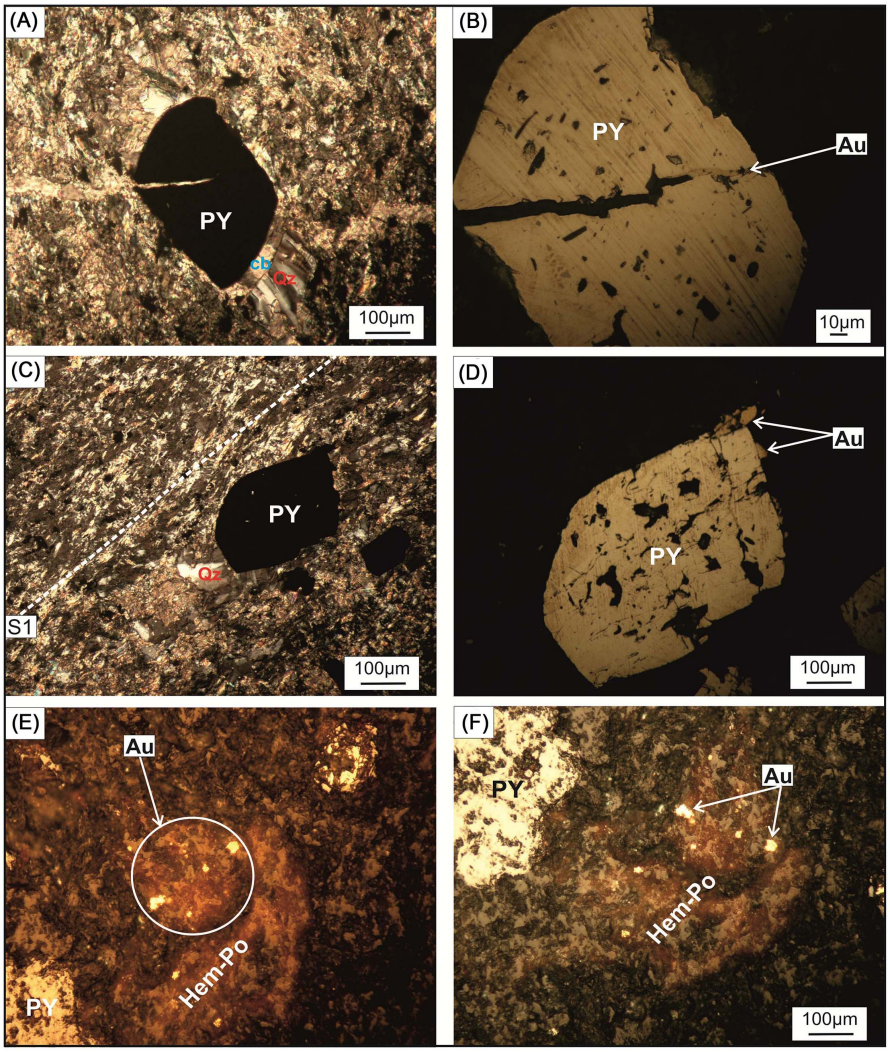

Figure 10. Microphotographs showing the relationship between Au and sulfides. (A) Image of a fractured pyrite at whose interfaces a quartz-carbonate-filled pressure shadow develops; (B) Gold grain filling the fractured pyrite; (C) Pyrite crystal developing a pressure shadow whose direction of growth is parallel to S1; (D) Gold grains precipitating on the faces of the pyrite crystal; (E) (F) Gold grains developing in the vicinity of pyrrhotite and hematite.

Gold mineralization is linked to hydrothermal fluid circulation from ductile to ductile-breaking to brittle stages ([41] [42] [43]). In fact, as the fluid rises, there is an interaction between the original minerals of the host rock and the fluid, and this is reflected at the time of crystallization by mineralogical assemblages related to this composition ([44]). This means that the hydrothermal fluids interacted with the Baguiomo basalts to remobilize the primary gold and all the other elements required to produce the various parageneses described above.

The paragenesis related to mineralization is controlled by the intensity of silicification and the pyritization phase. At Baguiomo, it is mainly the pyrite crystals at whose interfaces pressure shadows develop that contain the gold grains. Some players ([41] [42] [43] [45]) have demonstrated that these pressure sha-

dows are due to a subsequent reactivation of the micro-shear zones causing the latter to develop around the pyrite crystals. This reactivation must have caused a localized and repeated drop in pressure, inducing a reaction between the fluid and the host rock, followed by crystallization of the minerals in the spaces left behind.

Moreover, it is these openings that allow the fluid to enter and interact with the pyrite crystals already formed and the host rock, remobilizing the primary gold in the latter and then re-precipitating it within the latter ([43] [45]). This is in line with the work of ([39]) who have shown that there is primary gold in the basaltic rocks of Nassara.

The link between pyrite crystals and gold in country rocks is widely demonstrated in the West African craton ([4] [46]-[55]).

Based on this initial study, the Baguiomo zone is comparable to the Kwademen gold deposit ([7]), the Nassara gold deposit ([53]) and the Torkéra gold deposit ([56]). The gold in all these deposits is linked to pyrite crystals, and the shear deformation that controls mineralization is locally taken up by the second phase of deformation, which does not result in significant remobilization.

6. Conclusion

Gold mineralization at the Baguiomo gold mining site is hosted by basaltic formations cut by weakly to undeformed gabbro dykes. These basalts are affected by N-S to NNE-SSW-trending D1B shear deformation, which is locally picked up by the second phase of $D2_B$ deformation, a medium-trending NE-SW crenulation to brittle deformation. The basalts are thought to have been emplaced in an oceanic plateau setting, resulting from mantle plume activity. The primary gold mineralization associated with the accretion of these rocks would be capable of forming a deposit of around 5Moz after remobilization processes during the Eburnian orogeny. The gold is linked to pyrite crystals disseminated in the rock mass and to hematite, especially in the quartz vein concordant with $D1_B$. Gold associated with pyrite crystals is found in the pressure shadows developed during reactivation of the micro-shear zones.

Acknowledgements

The authors would like to thank the Bureau des Mines et de la Géologie du Burkina (BUMIGEB) for providing the total rock geochemical data for this study. The geochemical data were acquired during the SYSMIN 2003 project. Our thanks go to the authorities of the Geosciences and Environment Laboratory (LaGE) in the Geology Department at Joseph Ki Zerbo University, where the laboratory work was carried out.

Conflicts of Interest

The authors declare no conflicts of interest regarding the publication of this paper.

References

[1] Milési, J.P., Ledru, P., Feybesse, J.L., Dommanget, A. and Marcoux, E. (1992) Early Proterozoic Ore Deposits and Tectonics of the Birimian Orogenic Belt, West Africa. *Precambrian Research*, **58**, 305-344. https://doi.org/10.1016/0301-9268(92)90123-6

[2] Bourges, F., Debat, P., Tollon, F., Munoz, M. and Ingles, J. (1998) The Geology of the Taparko Gold Deposit, Birimian Greenstone Belt, Burkina Faso, West Africa. *Mineralium Deposita*, **33**, 591-605. https://doi.org/10.1007/s001260050175

[3] Hammond, N.Q., Robb, L., Foya, S. and Ishiyama, D. (2011) Mineralogical, Fluid Inclusion and Stable Isotope Characteristics of Birimian Orogenic Gold Mineralization at the Morila Mine, Mali, West Africa. *Ore Geology Reviews*, **39**, 218-229. https://doi.org/10.1016/j.oregeorev.2011.03.002

[4] Markwitz, V., Hein, K.A.A., Jessell, M.W. and Miller, J. (2016) Metallogenic Portfolio of the West Africa Craton. *Ore Geology Reviews*, **78**, 558-563. https://doi.org/10.1016/j.oregeorev.2015.10.024

[5] Goldfarb, R.J., André-Mayer, A.S., Jowitt, S.M. and Mudd, G.M. (2017) West Africa: The World's Premier Paleoproterozoic Gold Province. *Economic Geology*, **112**, 123-143. https://doi.org/10.2113/econgeo.112.1.123

[6] Masurel, Q., Eglinger, A., Thébaud, N., Allibone, A., André-Mayer, A.S., McFarlane, H., Miller, J., Jessell, M., Aillères, L., Vanderhaeghe, O., Salvi, S., Baratoux, L., Perrouty, S., Begg, G., Fougerouse, D., Hayman, P., Wane, O., Tshibubudze, A., Parra-Avila, L., Kouamélan, A. and Amponsah, P.O. (2022) Paleoproterozoic Gold Events in the Southern West African Craton: Review and Synopsis. *Mineralium Deposita*, **57**, 513-537. https://doi.org/10.1007/s00126-021-01052-5

[7] Lompo, M. (1991) Étude géologique et structurale des séries birimiennes de la région de Kwademen. Burkina Faso, Afrique de l'Ouest. (Evolution et contrôle des minéralisations sulfurées et aurifères, pendant l'Eburnéen). Blaise Pascal University, Clermont Ferrand II, Clermont-Ferrand.

[8] Feybesse, J.L., Billa, M., Guerrot, C., Duguey, E., Lescuyer, J.L., Milesi, J.P. and Bouchot, V. (2006) The Paleoproterozoic Ghanaian Province: Geodynamic Model and Ore Controls, Including Regional Stress Modeling. *Precambrian Research*, **149**, 149-196. https://doi.org/10.1016/j.precamres.2006.06.003

[9] Ouiya, P., Naba, S., Ilboudo, H., Sawadogo, S. and Yameogo, O. (2020) Mise en evidence de structures principales et connexes controlant la mineralisation dans le district aurifere de nassara au sud-ouest du Burkina Faso (Afrique de l'Ouest). *Journal des sciences*, **20**, 1-21.

[10] Chardon, D., Bamba, O. and Traoré, K. (2020) Eburnean Deformation Pattern of Burkina Faso and the Tectonic Significance of Shear Zones in the West African Craton. *BSGF—Earth Sciences Bulletin*, **191**, Article No. 2. https://doi.org/10.1051/bsgf/2020001

[11] Castaing, C., Billa, M., Milesi, J.P., Thieblemont, D., Le Metour, J., Egal, E., Donzeau, M., Guerrot, C., Cocherie, A., Chevremont, P., Tegyey, M., Itard, Y., Zida, B., Ouedraogo, I., Kote, S., Kabore, B.E., Ouedraogo, C., Ki, J.C. and Zunino, C. (2003) Notice explicative de la Carte géologique et minière du Burkina Faso à 1/1 000 000.

[12] Cathelineau, M., Boiron, M.C. and Tuduri, J. (2011) Fluides et genèse des concentrations minérales. *Géosciences*, *BRGM*, **13**, 56-63.

[13] Leube, A., Hirdes, W., Mauer, R. and Kesse, G.O. (1990) The Early Proterozoic Birimian Supergroup of Ghana and Some Aspects of Its Associated Gold Mineralization. *Precambrian Research*, **46**, 139-165. https://doi.org/10.1016/0301-9268(90)90070-7

[14] Oberthür, T., Vetter, U., Schmidt, M.A., Weiser, T., Amanor, J.A., Gyapong, W.A., Kumi, R. and Blenkinsop, T.G. (1994) The Ashanti Gold Mine at Obuasi, Ghana: Mineralogical, Geochemical, Stable Isotope and Fluid Inclusion Studies on the Metallogenesis of the Deposit. *Geologisches Jahrbuch D*, **100**, 31-129.

[15] Groves, D.I., Goldfarb, R.J., Gebre-Mariam, M., Hagemann, S.G. and Robert, F. (1998) Orogenic Gold Deposits: A Proposed Classification in the Context of Their Crustal Distribution and Relationship to Other Gold Deposit Types. *Ore Geology Reviews*, **13**, 7-27. https://doi.org/10.1016/S0169-1368(97)00012-7

[16] Béziat, D., Dubois, M., Debat, P., Nikiéma, S., Salvi, S. and Tollon, F. (2008) Gold Metallogeny in the Birimian Craton of Burkina Faso (West Africa). *Journal of African Earth Sciences*, **50**, 215-233. https://doi.org/10.1016/j.jafrearsci.2007.09.017

[17] Bessoles, B. (1977) Géologie de l'Afrique : Le craton Ouest Africain. Mém. B.R.G.M, Paris 88, 403 p.

[18] Pons, J., Barbey, P., Dupuis, D. and Léger, J.M. (1995) Mechanisms of Pluton Emplacement and Structural Evolution of a 2.1 Ga Juvenile Continental Crust: The Birimian of Southwestern Niger. *Precambrian Research*, **70**, 281-301. https://doi.org/10.1016/0301-9268(94)00048-V

[19] Gasquet, D., Barbey, P., Adou, M. and Paquette, J.L. (2003) Structure Sr-Nd Isotope Geochemistry and Zircon U-Pb Geochronology of the Granitoids of the Dabakala Area (Côte d'Ivoire): Evidence for a 2.3 Ga Crustal Growth Event in the Paleoproterozoic of West Africa? *Precambrian Research*, **127**, 329-354. https://doi.org/10.1016/S0301-9268(03)00209-2

[20] Doumbia, S., Pouclet, A., Kouamelan, A., Peucat, J.J., Vidal, M. and Delor, C. (1998) Petrogenesis of Juvenile-Type Birimian (Paleoproterozoic) Granitoids in Central Côte-d'Ivoire, West Africa: Geochemistry and Geochronology. *Precambrian Research*, **87**, 33-63. https://doi.org/10.1016/S0301-9268(97)00201-5

[21] Naba, S., Lompo, M., Debat, P., Bouchez, J.L. and Beziat, D. (2004) Structure and Emplacement Model for Late-Orogenic Paleoproterozoic Granitoids: The Tenkodogo-Yamba Elongate Pluton (Eastern Burkina Faso). *Journal of African Earth Sciences*, **38**, 41-57. https://doi.org/10.1016/j.jafrearsci.2003.09.004

[22] Vegas, N., Naba, S., Bouchez, J.L. and Jessell, M. (2008) Structure and Emplacement of Granite Plutons in the Paleoproterozoic Crust of Eastern Burkina Faso: Rheological Implications. *International Journal of Earth Sciences*, **97**, 1165-1180. https://doi.org/10.1007/s00531-007-0205-z

[23] Metelka, V., Baratoux, L., Naba, S. and Jessell, M.W. (2011) A Geophysically Constrained Litho-Structural Analysis of the Eburnean Greenstone Belts and Associated Granitoid Domains, Burkina Faso, West Africa. *Precambrian Research*, **190**, 48-69. https://doi.org/10.1016/j.precamres.2011.08.002

[24] Hirdes, W., Davis, D.W., Lüdtke, G. and Konan, G. (1996) Two Generations of Birimian (Paleoproterozoic) Volcanic Belts in Northeastern Côte d'Ivoire (West Africa): Consequences for the 'Birimian Controversy.' *Precambrian Research*, **80**, 173-191. https://doi.org/10.1016/S0301-9268(96)00011-3

[25] Vidal, M., Delor, C., Pouclet, A., Siméon, Y. and Alric, G. (1996) Geodynamic Evolution of West Africa between 2.2 and 2 Ga: the 'Archean' Style of the Green Belts and Birimian Sedimentary Assemblages of Northeastern Ivory Coast. *Bulletin de la Société Géologique de France*, **167**, 307-319.

[26] Pouclet, A., Vidal, M., Delor, C., Simeon, Y. and Alric, G. (1996) Birimian Volcanism in Northeastern Côte d'Ivoire: Evidence of Two Distinct Volcanotectonic Phases in Paleoproterozoic Geodynamic Evolution. *Bulletin de la Société Géologique de*

France, **167**, 529-541.

[27] Béziat, D., Bourges, F., Débat, P., Lompo, M., Martin, F. and Tollon, F. (2000) A Paleoproterozoic Ultramafic-Mafic Assemblage and Associated Volcanic Activity in the West African Craton. *Precambrian Research*, **10**, 25-47. https://doi.org/10.1016/S0301-9268(99)00085-6

[28] Baratoux, L., Metelka, V., Naba, S., Jessell, M.W., Grégoire, M. and Ganne, J. (2011) Juvenile Paleoproterozoic Crust Evolution during the Eburnean Orogeny (~2.2–2.0 Ga), Western Burkina Faso. *Precambrian Research*, **191**, 18-45. https://doi.org/10.1016/j.precamres.2011.08.010

[29] Feybesse, J.L., Milesi, J.P., Ouédraogo, M.F. and Prost, A. (1990) La « ceinture » protérozoïque inférieure de Boromo-Goren Burkina Faso: Un exemple d'interférence entre deux phases transcurrentes éburnéennes. *Comptes Rendus de l'Académie des Sciences*, **310**, 1353-1360.

[30] Ilboudo, H., Koffi, Y.H., Nanema, M., Wenmenga, U. and Lompo, M. (2015) A Stratiform (Cu-Zn ± Pb) Sulphide and Gold Occurrences in the Kwademen Birimian System (Burkina Faso, West Africa). *Asian Academic Research Journal of Multidisciplinary*, **2**, 1-23.

[31] Middlemost, E.A.K. (1994) Naming Materials in the Magma/Igneous Rock System. *Earth-Science Reviews*, **37**, 215-224. https://doi.org/10.1016/0012-8252(94)90029-9

[32] Jensen, L.S. (1976) A New Cation Plot for Classifying Sub-Alkalic Volcanic Rocks. *Ontario Division Mines Miscellaneous Paper No.* 66.

[33] Miyashiro, A. (1974) Volcanic Rock Series in Island Arcs and Active Continental Margins. *American Journal of Science*, **274**, 321-355. https://doi.org/10.2475/ajs.274.4.321

[34] Lompo, M. (2009) A Model of Subsidence of an Oceanic Plateau Magmatic Rocks in the MaleonShield of the West African Craton Geodynamic Evolution of the 2.25-2.0 Ga Paleoproterozoic. In: Reddy, S.M., Mazumder, R., Evans, D.A.D. and Collins, A.S., Eds., *Paleoproterozoic Supercontinents and Global Evolution*, Geological Society, London, 231-254.

[35] McDonough, W.F. and Sun, S.S. (1995) The Composition of the Earth. *Chemical Geology*, **120**, 223-253. https://doi.org/10.1016/0009-2541(94)00140-4

[36] Augustin, J., Gaboury, D. and Crevier, M. (2017) Structural and Gold Mineralizing Evolution of the World-Class Orogenic Mana District, Burkina Faso: Multiple Mineralizing Events over 150 Million Years. *Ore Geology Reviews*, **91**, 981-1012. https://doi.org/10.1016/j.oregeorev.2017.08.007

[37] Goldfarb, R.J., Groves, D.I. and Gardoll, S. (2001) Orogenic Gold and Geologic Time: A Global Synthesis. *Ore Geology Reviews*, **18**, 1-75. https://doi.org/10.1016/S0169-1368(01)00016-6

[38] Velasquez, G., Beziat, D., Salvi, S., Tosiani, T. and Debat, P. (2011) First Occurrence of Paleoproterozoic Oceanic Plateau in the Guiana Shield: The Gold-Bearing El Callao Formation, Venezuela. *Precambrian Research*, **186**, 181-192. https://doi.org/10.1016/j.precamres.2011.01.016

[39] Ouiya, P., Yaméogo, A.O., Ilboudo, H. and Naba, S. (2022) Implication of Paleoproterozoic Basalt Fertility Related to Mantle Plume Activity in Nassara Gold Mineralization (Burkina Faso, West Africa). *Open Journal of Geology*, **12**, 1013-1031. https://doi.org/10.4236/ojg.2022.1211048

[40] Phillips, G.N., Groves, D.I. and Brown, I.J. (1987) Source Requirements for the Golden Mile, Kalgoorlie: Significance to the Metamorphic Replacement Model of Archean Gold Deposits. *Canadian Journal of Earth Sciences*, **24**, 1643-1651.

https://doi.org/10.1139/e87-158

[41] Goldfarb, R.J., Baker, T., Dubé, B., Groves, D.I., Hart, C.J.R. and Gosselin, P. (2005) Distribution, Character, and Genesis of Gold Deposits in Metamorphic Terran. In: Hedenquist, J.W., Thompson, J.F.H., Goldfarb, R.J. and Richards, J.P., Eds., *One Hundredth Anniversary Volume* 1905-2005. https://doi.org/10.5382/AV100.14

[42] Bons, P.D., Elburg, M.A. and Gomez-Rivas, E. (2012) A Review of the Formation of Tectonic Veins and Their Microstructures. *Journal of Structural Geology*, **43**, 33-62. https://doi.org/10.1016/j.jsg.2012.07.005

[43] Velasquez, G., Béziat, D., Salvi, S., Siebenaller, L., Borisova, A.Y., Pokrovski, G.S. and De Parséval, P. (2014) Formation and Deformation of Pyrite and Implications for Gold Mineralization in the El Callao District, Venezuela. *Economic Geology*, **109**, 457-486. https://doi.org/10.2113/econgeo.109.2.457

[44] Jébrak, M. and Marcoux, E. (2008) Géologie des ressources minerals. Ministère des ressources naturelles et de la faune.

[45] Velasquez, G., Salvi, S., Siebenaller, L., Béziat, D. and Carrizo, D. (2018) Control of Shear-Zone-Induced Pressure Fluctuations on Gold Endowment: The Giant El Callao District, Guiana Shield, Venezuela. *Minerals*, **8**, Article 430. https://doi.org/10.3390/min8100430

[46] Fougerouse, D., Micklethwaite, S., Miller, J., Ulrich, S. and McCuaig, T.C. (2015) WITHDRAWN: The Obuasi Gold Deposit, Ghana: A West African Giant. *Ore Geology Reviews*, **50**, 665-675. https://doi.org/10.1016/j.oregeorev.2015.06.019

[47] Traoré, Y.D., Siebenaller, L., Salvi, S., Béziat, D. and Bouaré, M.L. (2016) Progressive Gold Mineralization along the Syama Corridor, Southern Mali (West Africa). *Ore Geology Reviews*, **78**, 586-598. https://doi.org/10.1016/j.oregeorev.2015.11.003

[48] Augustin, J., Gaboury, D. and Crevier, M. (2016) The World-Class Wona-Kona Gold Deposit, Burkina Faso. *Ore Geology Reviews*, **78**, 667-672. https://doi.org/10.1016/j.oregeorev.2015.10.017

[49] Lawrence, D.M., Lambert-Smith, J.S. and Treloar, P.J. (2016) A Review of Gold Mineralization in Mali. In: Bouabdellah, M. and Slack, J., Eds., *Mineral Deposits of North Africa*, Springer, Cham, 327-351. https://doi.org/10.1007/978-3-319-31733-5_13

[50] McCuaig, T.C., Fougerouse, D., Salvi, S., Siebenaller, L., Parra-Avila, L.A., Seed, R., Béziat, D. and André-Mayer, A.S. (2016) The Inata Deposit, Belahouro District, Northern Burkina Faso. *Ore Geology Reviews*, **78**, 639-644. https://doi.org/10.1016/j.oregeorev.2015.11.014

[51] Salvi, S., Sangaré, A., Driouch, Y., Siebenaller, L., Béziat, D., Debat, P. and Femenias, O. (2016) The Kalana Vein-Hosted Gold Deposit, Southern Mali. *Ore Geology Reviews*, **78**, 599-605. https://doi.org/10.1016/j.oregeorev.2015.10.011

[52] Salvi, S., Velásquez, G., Miller, J.M., Béziat, D., Siebenaller, L. and Bourassa, Y. (2016) The Pampe Gold Deposit (Ghana): Constraints on Sulfide Evolution during Gold Mineralization. *Ore Geology Reviews*, **78**, 673-686. https://doi.org/10.1016/j.oregeorev.2015.11.006

[53] Ouiya, P., Siebenaller, L., Salvi, S., Béziat, D., Naba, S., Baratoux, L., Naré, A. and Franceschi, G. (2016) The Nassara Gold Prospect, Gaoua District, Southwestern Burkina Faso. *Ore Geology Reviews*, **78**, 623-630. https://doi.org/10.1016/j.oregeorev.2015.11.026

[54] Amponsah, P.O., Salvi, S., Béziat, D., Baratoux, L., Siebenaller, L., Nude, P.M., Nyarko, R.S. and Jessell, M.W. (2016) The Bepkong Gold Deposit, Northwestern Ghana. *Ore Geology Reviews*, **78**, 718-723.

https://doi.org/10.1016/j.oregeorev.2015.06.022

[55] Ouattara, S.A., Yacouba, C. and Kouadio Fossou, J.L.H. (2017) Les Altérations Hydrothermales Associées À La Minéralisation Aurifère Du Gisement De Dougbafla (District d'Oumé-Hiré, Centre-Ouest De La Côte d'Ivoire). *European Scientific Journal*, **13**, 108-125. https://doi.org/10.19044/esj.2017.v13n30p108

[56] Ouédraogo, B.F. (2021) Evolution de la teneur en or le long du corps minéralisé Dans le gite aurifère de Torkera, district de Gaoua: Déformation, géochimie et altération hydrothermale. Master's Thesis, Université Joseph KI Zerbo, Ouagadougou.